MECHANICS.— **A study of the topology of a laser - damaged surface**, by *Pericles S. Theocaris**, *Institute of Mechanics,* National Academy of Athens.

ABSTRACT

We consider scattering from an initially plane surface of a thin plexiglas plate damaged by an impinging coherent light beam of a laser. The morphology and the characteristic dimensions of the damage speckles was studied during the evolution of the phenomenon by interferometry and the creation of diffraction patterns. The cusped interferogram created by superposition of the evoluting two initial diffraction patterns, created during two successive damage steps, forms caustics corresponding to **hyperbolic umbilic catastrophes.** *An experimental study of the evolution of the damage phenomenon clarifies the mechanisms of elastic and plastic deformations of the affected zone.*

INTRODUCTION

Laser beams are capable of producing interesting and useful effects. Investigations of the effect of laser beams have multiplied over the recent years. By laser effects we mean here the interactions between high-power laser beams and matter. As a consequence of this interaction, phenomena of heating, melting, vaporization and plasma production may be created. Some of the most interesting phenomena associated with lasers involve effects produced when a high-power laser beam is absorbed at an opaque surface.

The temperature rise, produced by the absorbed flux of the impinging light beam on an opaque surface, if this flux is below the levels producing melting and vaporization of the substrate, may be evaluated by a classical thermodynamic formalism. Indeed, we can regard the optical energy as being instantaneously turned into heat at the point at which the light is absorbed. Since the heat distribution occurs instantaneously for each laser pulse, a local equilibrium is established, fact which justifies the application of usual equations of heat flow. This theory ceases to be valid only for pulsed lasers with a picosecond duration of the pulse. Then, for lasers operating in a mode-locked condition, it is common use to simply integrate over several pulses

* Π. ΘΕΟΧΑΡΗ, Μελέτη τῆς τοπολογίας ἐπιφανειῶν ὑπὸ τὴν ἐπίδρασιν ἀκτίνων Laser.

and rise a smooth envelope of the mode-locked train as a pulse shape for temmerature calculations. During the calculations of the temperature rise it is a good approximation to assume that the thermal properties of the absorbing material are independent of the temperature. In this case it is also assumed that the energy lost from the surface through reradiation or convection is negligible. For long pulses, or for lasers of continuous emission, heat can be conducted over a large area, which contributes to a reradiation even for low levels of power concentration. In this case, the large area influenced by the impinging energy contributes significantly to a heat loss.

For many cases of practical interest we may regard the problem as one-dimensional, that it is assumed that the transverse dimensions of the laser beam are large compared to the depth to which heat is conducted. Furthermore, it has been established that for many types of laser, the laser pulse, normalized to unity at its peak, has approximately the same shape, when considered as a function of its duration. This shape is generally accepted as a standard for normal emissions. This shape, of an unsymmetric bell-form, presents a maximum at a laser pulse duration equal to 0.2 the normalized pulse duration.

The first phase of the phenomenon of absorption of laser radiation, which is described as *heating* of the surface of the material in the regime where no phase transformation occurs, is followed by a second phase, which corresponds to a higher regime of absorbed flux densities, creating *melting* of surfaces absorbing laser radiations. This phase is followed by a third one when *vaporization* of the material of the surface takes place. The situation of melting, without vaporization, is produced only over a fairly narrow range of laser parameters. Indeed, the flux density must be high enough to raise the surface above the melting point, but not much higher, sufficient to excite the material to vaporize. For normal lasers, with a careful control over the parameters of the laser, reasonable melting can be obtained, although the depths melted are generally limited. For continuous high-power lasers any desired duration of exposure can be attained by shuttering, and therefore effective melting can be produced. Therefore, for laser melting with a maximum penetration, continuous lasers may be the most feasible solution.

There is a great difference in the behaviour of surfaces struck by different laser pulses depending on their duration times. Typically very-high-power short pulses do not produce much vaporization, but instead, remove only

a small amount of material from the surface, whereas longer lower-power pulses from normal-pulse lasers produce deep narrow holes in the material.

At low laser flux densities, the amount of vaporized material depends more on the thermal conductivity of the material, than on the latent heat of vaporization. As the laser flux density increases, it reachers a value at which the heat is supplied too fast to be conducted away. Then, the dominant factor becomes the latent heat of vaporization. Considering that the latent heat of typical materials used in such procedures is much smaller than either the latent vaporization, or the quantity of heat required to raise the temperature to the boiling point of the material, then, it is reasonable to neglect the influence of the liquid phase created during lased attack, fact which simplifies considerably the calculations.

However, in many cases much of the material is removed in the liquid state rather that in the vaporized state. The molten material on the walls of the perturbation, ejected because of the pressure, increases the amount of the material removed and eventually creates a blowoff phenomenon, when the blowoff material is emitted from the surface by the laser heating. The molten and resolidified material is concentrated at the rim around the lip of the shallow crater, and this phenomenon is clearly indicated in the experiments presented in this paper. Moreover, this material is contributing a significant amount to the volume of material removed from the crater.

The blowoff material created during the early stages of the action of the laser beam develops a recoil pressure, which raises the boiling point of the target, above the usual vaposization temperature. This increase in vaporization temperature of the vaporized material is sufficiently high, so that the surface is prevented from vaporizing further and the material continues to heat to a high temperature above the normal vaporization temperature, as further laser light is absorbed at the target surface. Eventually, the target surface will reach a critical point, where vaporization can occur. Although the surface of the target is effectively cut off from the incoming radiation for a large fraction, since the energy in the pulse is continuously absorbed by material in front of the surface, at the end of the pulse· the blowoff material becomes progressively very hot and it begins to reradiate thermally, fact which causes further vaporization.

Modern methods of processing materials are actually using the above described phase of the laser beam effects for industrial and scientific appli-

cations. Indeed, this *directed energy source* concept has provided means for performing such operations without intimate contact between the energy source and the workpiece, fact which raises the attractive possibility of eliminating knives, drills, flames, chemicals and other instruments, from certain delicate operations in various fields of physical and applied sciences, as well as in medical sciences.

While the already mentioned phenomena, created by using convenient laser beams constitute the basic ones, there are also some further additional phenomena, which are intimately related, being consequences of the particular state of action of a certain laser beam on a certain material. These phenomena are mainly the sputtering during evaporation, the evaporation of entrapped water, the heating of entrapped gases, chemical reactions, phase changes, shock wave propagation and plasma production, when a laser radiation strikes a solid target. All these phenomena have been extensively studied in the numerous publications and the existing literature related to this interesting chapter of science.

On the other hand, the scattering of ion beams from solid surfaces can give useful information about this particle (ion)- solid interaction [1]. It is accepted as a good approximation for describing the phenomenon of interaction of ion-solid surface that the interaction potential between ion and solid is zero outside a surface Σ considered as roughly flat, but is perturbed in a random manner by thermal effects due to speckles created by a laser-beam damage. An eikonal approximation of the exact quantum scattering from the surface Σ is described by the model introduced by Garibaldi et al. [2] for special forms of surface Σ based of the theory of the *classical surface rainbow* studied by Smith et al. [3].

In this paper, by assuming more realistic flat surfaces, we establish the topology of the classical rainbow in the two-dimmensional space of directions of the scattered particles. In was found that the rainbow in such a space consists of two caustics [4], one inside the other. The inner curve has the form of a cuspoid curve with several cusps, while the outer curve is a smooth one. Furchermore, the diffraction spots lying near rainbows appear intense and distinct near cusps and become softened to almost smooth curves far away from them. Employing Kirchhoff diffraction theory we have neglected as insignificant multiple reflections between different parts of the surface, assump-

tion which is justified for our case where the total variation $\Delta\Theta$ of the speckled slopes is small and the incident light beam does not graze the surface.

A series of tests were executed on thin flat plexiglas plates, whose initial average surface was roughly flat. A collimated light beam, emitted from an CW Argon-ion laser, was impinging the surface. By increasing the energy flux, emitted from the laser beam, speckles on the surface of the plate were created, whose areas are extended as the light flux is increased. The topography of the disturbances was defined by a series of interferograms formed on a reference screen placed some distance from the workpiece, so that the reflected-light beam from the speckled region to be received on this screen. Additional measurements of the deformed by the speckles lateral surfaces of the workpiece were performed by using a rectilinear surface graph-recorder of the Talysurf type, whose very fine stylus scans the surface of the testpiece along parallel lines at different orientations. Interesting results were derived, where the experimental data confirm the validity of the theory and establish the laws of deformation of a surface under the influence of a laser light beam.

THEORY

We consider scattering from a local corrugation, created by a laser damage, on a flat surface Σ of a hard opaque material. Simplified diffraction theory enables to study diffraction effects, and incoherence to be treated within the same framework. The *classical rainbow* is a curve C in the two-dimensional space of the deflections G of impinging light on the surface of a perturbation. A topological study of cerves C shows that C has cusps, whose position depend on the form of the surface studied Σ. Moreover, the scattering of light in the perturbation is singular on Σ, with the singularities there softened by diffraction. The diffraction functions may be described along their smooth parts, as well as at the cusps of G.

The surface Σ under examination is considered as perfectly flat, containing a random perturbation, because of the inelastic effects created by thermal influence, due to an impinging laser beam. The topology of the classical rainbow in the image domain consists of two caustics, one inside the other, in which the inner curve has several cusps, while the outside curve is a smooth one.

We use a simpler version of a rippling-mirror model, in order to derive a simple approximate formula describing the pattern, according to which multiple reflections between different parts of the surface are neglected as

insignificant, since surface slopes are small and the incident beam is normally impinging the flat surface. Therefore, the angle variation, $\Delta\Theta$, does not exceed a few degrees.

We consider a system of Cartesian coordinates $\mathbf{r}=r\ (x,y,z)$, for which the plane $z=0$ defines the horizontal plane of the reflector, whose points are located by $\mathbf{R}=(x,y)$ and the rippled surface under study is defined by $h(\mathbf{R})$ above the plane $\mathbf{R}$, where h expresses the height of the perturbation.

The incident beam is expressed by a single plane wave $\psi\ (r,t)$ of frequency ω_0, corresponding to an energy $E_0=h\omega_0$ and a wavevector $\mathbf{k}_0$. Its wavelength is given by:

$$\lambda_0 = \frac{2\pi}{k_0} = \frac{h}{(2mE_0)^{1/2}}$$

where m is the mass of the particles. The horizontal component of k_0 is k_h and k_n the vertical, which is negative, since the wave is approaching Σ from above. Finally, the amplitude of the wave is denoted by a, which is specified by $\mathbf{k}$ and ω. Indeed, the scattered particles emerge in different directions $\mathbf{k}$ and with different frequencies ω, because of the shifts due to Doppler effect, caused by the time dependence of h. Therefore, they may be represented by a wavefunction, which is a sheaf of plane waves receding from Σ, so that their vertical component k_n is positive real for $K<k$ and positive imaginary, if $K>k$.

For a periodic lattice of disturbances, where the scattering is elastic $(\omega=\omega_0)$ the light intensity I is expressed by [5]:

$$I(k_0, \omega_0; k, \omega) = \delta(\omega-\omega_0) \sum_G |S_G|^2 \delta(k-k_0-C) \qquad (1)$$

This relation indicates that the emergent particles appear as a series of diffracted beams on directions $k=k_0+G$, where G are two-dimensional vectors of the reciprocal surface lattice and the strength of the Gth diffracted beam is expressed by $|S_G|^2$. Then, the diffraction amplitude S_G is given by:

$$S_G = \frac{1}{A} \iint_{cell} d\mathbf{R} \exp\left\{ -i \left[\mathbf{G}\cdot\mathbf{R} + (|k_{0n}|+k_n)\, h(\mathbf{R}) \right] \right\} \qquad (2)$$

In this relation A expresses the area of the unit cell. For λ and h small, the number of the observed diffracted beams is expressed by:

$$N = \frac{mAE_0}{2\pi h^2} \tag{3}$$

and is large, so that the diffracted beams are densely distributed in direction Moreover, the respective deflection $\mathbf{G}=(\mathbf{k}-\mathbf{k}_0)$ may be regarded as a quasi-continuous variable. But, when $k_0=k$ is large, the integrand of Eq. (2) is rapidly oscillating, as **R** traverses the unit cell, and most of the area of integration gives no contribution, because of destructive interference, except isolated points $R_i(\mathbf{k}_0, \mathbf{G})$, where the phase of the integrand is stationary and where we obtain contributions to S_G. The station·ry points R_i are given by:

$$G = -(|k_0|+k_z)\nabla h(R_i) \tag{4}$$

Relation (4) expresses the condition that the surface point **R** reflects a classical particle specularly from $\mathbf{k}_0$ to $(\mathbf{k}_0+\mathbf{G})$. Therefore, it may be established that only classical paths contribute to the diffraction integral of Eq. (2), when k_0 is large and relation (4) constitutes an implicit equation for G, since it is valid that:

$$k_z = [k^2 - (K_0+G)^2]^{1/2}$$

Then, the dependence of k_z on **G** is **weak** for gently varying surfaces S, as it is the case with the perturbations considered here, when the points R_i are sufficiently separate between them. We could therefore expand the phase in Eq. (2) up to squares of terms $(\mathbf{R}-\mathbf{R}_i)^2$ and we derive the expression for the diffraction amplitudes S_G given by:

$$S_G = \frac{2\pi}{A(|k_{0z}|+k_z)} \sum_i \gamma_i \frac{\exp\{-i[\mathbf{G}\cdot\mathbf{R} + (|k_{0z}|+k_z)\, h(\mathbf{R}_i)]\}}{\{|\mathcal{K}(R_i)|\}^{1/2}} \tag{5}$$

where the summation is over all points R_i, which are reflecting points with deviation **G**. Finally, γ_i takes the values $\gamma_i=i$ for a minimum, $\gamma_i=-i$ for a maxi-

mum and $\gamma_i = 1$ for a saddle point. For gently varying surfaces Σ, $K(\mathrm{R})$ is the Gaussian curvature of Σ at **R**, that is the product of the two principal curvatures at **R** and it is positive for Σ concave or convex and negative for Σ saddle-shaped.

What is observed in experiments is $|S_G|^2$. Equation (5) in the extreme limit indicates that experiment would datect only an average of the interference oscillations, which are tending to zero, while it remains a steady term. Then, Eq. (5) gives:

$$|S_G|^2_{clas} = \frac{4\pi^2}{A^2(|k_{0z}|+k_z)^2} \sum_i \frac{1}{|\mathcal{K}(R_i)|} \tag{6}$$

which indicates that the Gaussian curvature of Σ at **R** yields an inverse measure of the strength contribution from the path i.

For a given $\mathbf{K}_0$, the intensity scattered with deflection **G** becomes infinite whenever any contributing surface point $R_i(\mathbf{G}, \mathbf{K}_0)$ lies in vanishing points $\mathbf{K}(\mathbf{R})$. Then, the equation:

$$\mathcal{K}(\mathbf{R}) = \frac{\partial^2 h}{\partial x^2}\frac{\partial^2 y}{\partial y^2} - \left(\frac{\partial^2 h}{\partial x \partial y}\right)^2 = 0 \tag{7}$$

defines a line L on this surface, whose image point **G** lies on a respective line C, which is strongly illuminated and constitutes a *caustic* in the **G**-plane, that is the locus of rays for which angular focussing occurs and the observed scattering should be dominated by this line C on **G**. The respective lines C are called the *rainbow lines*. Along these lines lie the most densely distributed diffraction spots, fact which justifies their names [4]. Figure 1 presents the configuration of the surfaces **G** in space.

According to relation (7) the surface Σ, that is the landscape above the **R**-plane, will have *summits*, where strong repulsive forces are exerted by the incoming particles, *immits*, where minima of the repulsive forces exist, as well as saddle points [6]. Now, the lines L are the points of zero Gaussian curvature, where one of the two principal curvatures of Σ vanishes, while at the summits or immits both curvatures are either positive or negative. Therefore, between a saddle and a summit, or an immit, lines L must cross an impair number of times, the least being one.

Thus, lines L consist of closed curves surrounding regions of positive K containing summits and immits, while the open region of negative curvature containing saddles. The curve L_1 around summits will generally not have the same shape as the curves L_2 arount immits, because summits and immits are not symmetrical features of Σ.

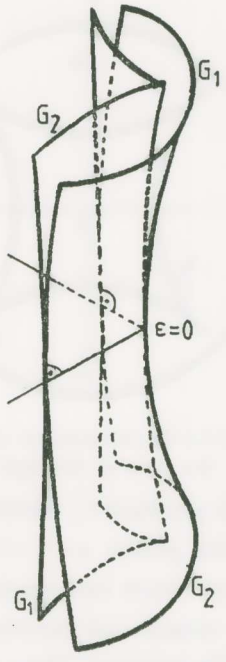

Fig. 1 Schematic of the hyperbolic umbilic caustic surfaces.

While the rainbow line C in **G** is generated by L of Eq. (4), the two closed curves L_1 and L_2 are generating two closed curves C_1 and C_2 in **G** respectively, where C_2 lie within C_1. Figure 2 presents a general form of rainbow lines C_1 and C_2 originating near summits and immits of the surface Σ. From relation (4) it can readily be found that the image of C is a single rectangle given by:

$$G_x = \pm \frac{2\pi h_p}{a} (|k_0|+k_z) \tag{8}$$

where a and b are the interlattice distances and h_p for an initially flat surface is expressed by:

$$h_p = \varepsilon\, h_p(\mathbf{R}) = h_0 \cos\left(\frac{2\pi x}{a}\right)\cos\left(\frac{2\pi y}{b}\right) \tag{9}$$

where ε is the elevation due to the perturbation, which is not symmetrical in summits and immits. Then, for ε different than zero, the rectangular rainbow line, given by Eqs. (8), must split into two different curves, as indicated in Fig. 1. Using catastrophe theory [7], we state that singularities in the two-

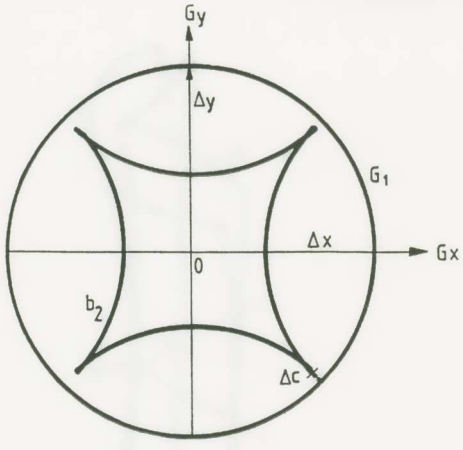

Fig.2 The caustic curves derived by the intersection of the caustic surfaces by a plane normal to the axis of the light bundle.

dimensional case of plane **G** are lines C, which are smooth except at cusps, whose simplest cases are the points $x=y=0$ on the curve $y^2=x^3$.

The rainbow surface must have two sheets C_1 and C_2, which are touching each other along $\varepsilon=0$, at a corner, and therefore these catastrophes are of the type of the *hyperbolic umbilic* surfaces. Thus, we expect the rainbow lines to take the form shown in Fig. 2. Then, it is easy to derive that:

$$\Delta c \approx \frac{16\pi^2\varepsilon^2 h_0\sqrt{2}}{a\lambda_0} \quad \text{and} \quad \Delta x \approx \frac{16\pi^2\varepsilon\, h_0}{a\lambda_0}, \quad \Delta y \approx \frac{16\pi^2\varepsilon\, h_0}{b\lambda_0} \tag{10}$$

However, diffraction effects obscure the details of the rainbow line C, because G is an intermittent variable, consisting of a series of reciprocal lattice points. Interference between waves emerging from different points in the same lattice cell in **R** blurs out the rainbow line into a diffraction pattern in **G**, while interference between waves emerging from equivalent points in different cells quantizes **G**, so that this diffraction pattern is sampled at discrete points. Figure 3 presents the contours of the cusp diffraction function $|C|^2$ given by relation (13).

Near a smooth portion of the rainbow line C relation (5) breaks down, since two contributing surface points $\mathbf{R}_1$ and $\mathbf{R}_2$ coalesce. In such a case it

is necessary to establish a uniform approximation to S_G^R, based on Eq. (2), which is valid on and near the line C, while relation (5) is valid far away from C. In this case the result is that the contribution S_G^R from $\mathbf{R}_1$ and $\mathbf{R}_2$ in Eq. (5) must be replaced by an approximate formula involving Airy functions A_i [8] and their derivatives A_i.

The diffraction amplitude S_G^R near the rainbow line is given by [4]:

$$S_G^R = \frac{2\pi\sqrt{\pi}\,\exp\left[\frac{1}{2}i\left(\Phi_1+\Phi_2-\frac{3}{2}\pi\right)\right]}{A(|k_{0z}|+k_z)}\left[\left(\frac{1}{\mathcal{K}_1^{1/2}}+\frac{1}{(-\mathcal{K}_2)^{1/2}}\right)\left(\frac{3(\Phi_2-\Phi_1)}{4}\right)^{1/6} \times A_i\left[-\frac{3}{4}(\Phi_2-\Phi_1)^{2/3}\right] - i\left(\frac{1}{\mathcal{K}_1^{1/2}}-\frac{1}{(-\mathcal{K}_2)^{1/2}}\right)\left(\frac{4}{3(\Phi_2-\Phi_1)}\right)^{1/6} \times A_i'\left[-\left(\frac{3}{4}(\Phi_2-\Phi_1)\right)^{2/3}\right]\right] \tag{11}$$

where Φ denotes the phase in Eq. (5) expressed by:

$$\Phi \equiv -\left[\mathbf{G}\cdot\mathbf{R} + (|k_{0z}|+k_z)\,h(\mathbf{R})\right] \tag{12}$$

For a convenient selection of the signs of the Gaussian curvatures K_1 and K_2 and positive roots for $(\Phi_2-\Phi_1)^{2/3}$ the Airy functions have a negative argument and are thus oscillatory functions [9]. In this case relation (11) describes the *supernumerary rainbows* [10]. For deflections G on the dark side of C, there are no real paths $\mathbf{R}_1$ and $\mathbf{R}_2$ and taking a real negative root of $(\Phi_2-\Phi_1)^{2/3}$ the Airy functions have a positive argument and decay exponentially into the shadow. Figure 4 presents the refraction caustics from a laser speckle on a plexiglas plate. Fig. 4a gives a general view of the pattern, while Fig. 4b the detail of the inner caustic C_2.

Finally, along the rainbow line C, relation (11) remains finite and tends to the value of order $(h_0/\lambda_0)^{1/3}$, larger that the classical region away from C, where h_0 expresses the maximum excursion of Σ from the R-plane. On the other hand, near a cusp of C, where three points R_i are coalescing there, relation (11) breaks down and, instead of Airy functions, we must use the following function describing the diffraction near the cusp catastrophe of the third order [11].

$$C(x,y) \equiv \int_{-\infty}^{\infty} \exp\left[i\left(\frac{t^4}{8}-\frac{xt^2}{2}+yt\right)\right]dt \tag{13}$$

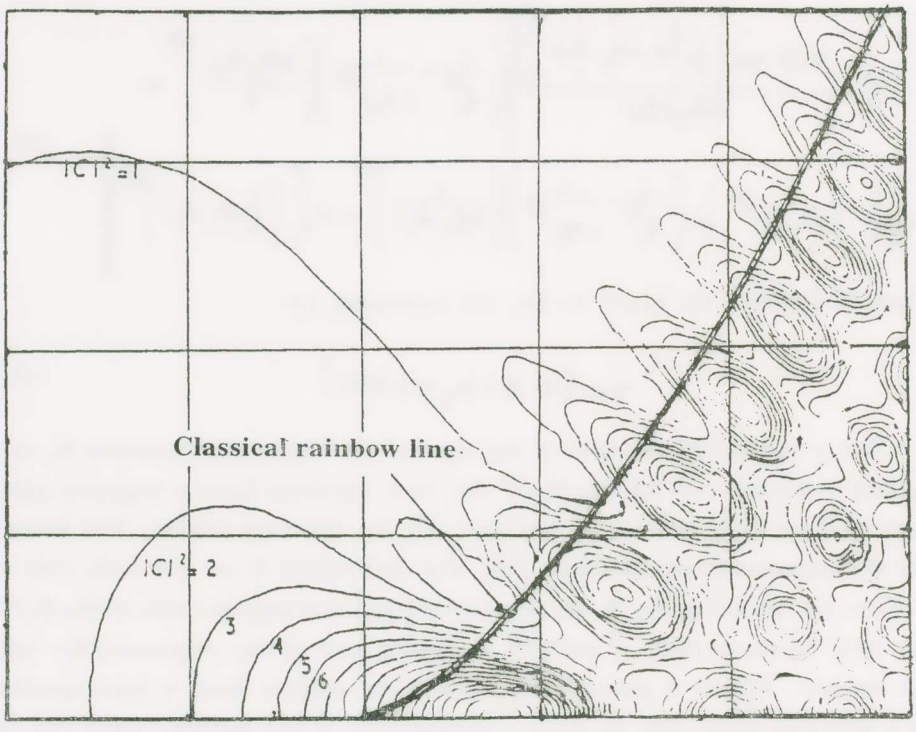

Fig. 3 The diffraction pattern at the vicinity of a casp of the internal caustic C_2 where the classical rainbow line is developed.

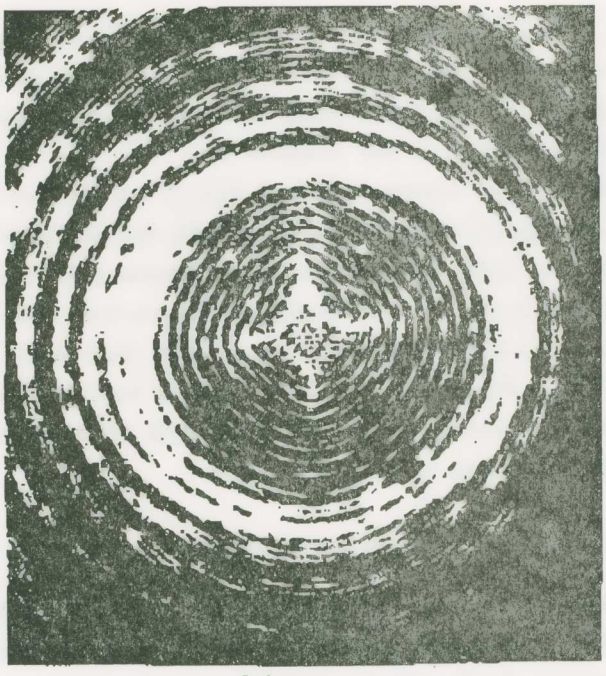

(a)

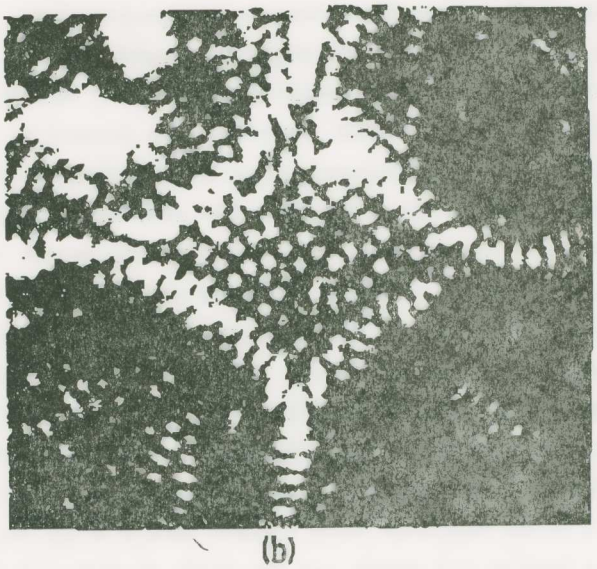

(b)

Fig.4 (a) Interferogram of the reflected rays from the speckle created by a laser beam and the pair of caustics formed by the diffraction patterns of the interferograms. (b) Detail of the inner cuspoid caustic C_2.

where the x, y-variables are smooth distortions of G_x and G_y. It turns out that on the cusp itself the quantity $|S_G|^2$ rises to a value of order $(h_0/\lambda_0)^{1/2}$, larger than in the classical region away of C, so that the cusps are the most strongly diffracting parts of the rainbow line.

Figures 4-6 present contour maps of $|C(x,y)|^2$ at different steps of evolution of the damage phenomenon on an initially flat plexiglas plate attacked by an Argon-Laser light beam. In the same figures a quantization of equivalent points, which are not sufficiently closely packed, creates distinct diffraction spots on G appearing along the rainbow lines and especially near the cusps. While in Fig. 4 the laser light beam is impinging normally to the flat surface, the patterns in Figs. 5 and 6 are with different amounts of obliqueness of the impinging light rays.

LASER DAMAGE OF SURFACES STUDIED BY FRAUNHOFER DIFFRACTION

On the basis of Babinet's principle [5], it can be shown that the radiation reflected from an infinite perfectly reflecting surface containing a speckle of a few microns depth, which works as a total absorber, produces the same diffraction pattern as the radiation propagating in the opposite direction through a hole of the same dimensions in an opaque plate.

A speckle, many microns deep, might be considered as a total absorber and hence scattering from its pit might reasonably be expected to result in a single-opening diffraction pattern. Since the pits created by speckles developed during the first and subsequent phases of laser damage are always shallow, their depth being of the order of a few microns, as compared to their surface dimensions, a simple model for such a system would be to consider the *diffraction of radiation,* reflected from the surface of the specimen, and the bottom of the pit. Since the morphology of the pit is with abrupt slopes at the periphery, like a shallow crater, it is possible to ignore the effect of scattering from the sides of the pit. Therefore, the part of radiation reflected from the base of the pit can be considered shifted in phase relatively to the part of radiation reflected from the surface of the specimen by an amount of 2kd where k is the radiation wave number and d is the depth of the pit. This model is a typical and simple one for single grooves and diffraction gratings [12]. More rigorous theories exist for geometries of the discontinuity close to the reasonance domain. However, since the pits created by laser da-

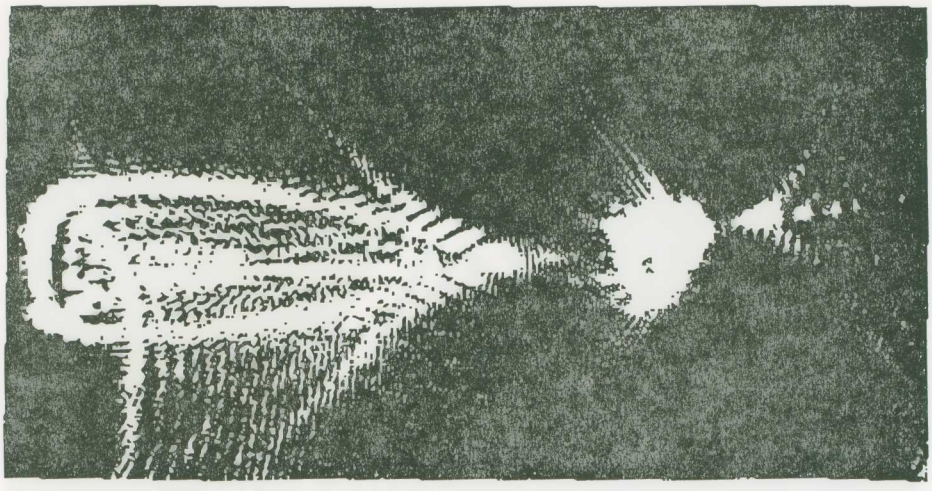

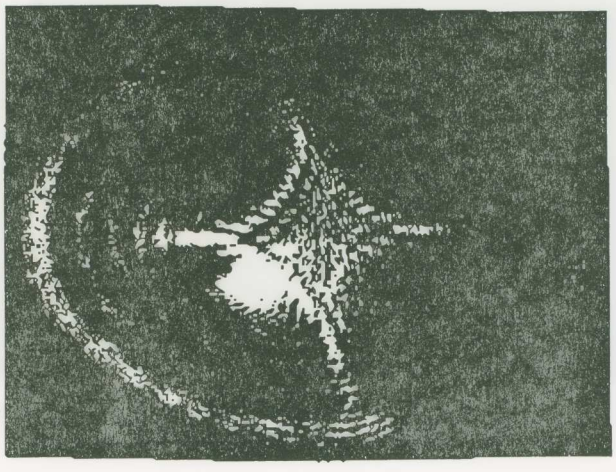

Fig.5 The same patterns as in Fig. 4 but under different angles of incidence of the light bundles on the reference screen.

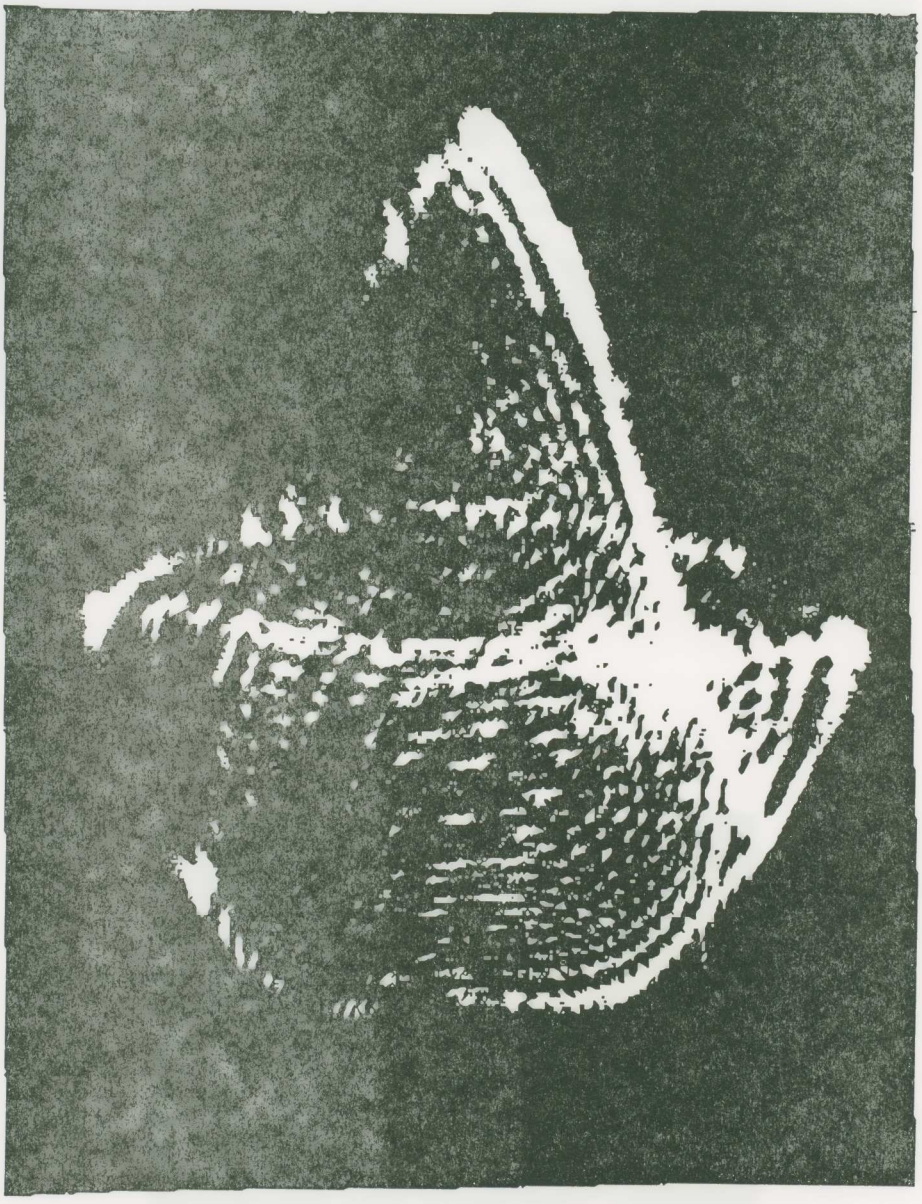

Fig. 6 The same pattern under large angles of inclination of the references screen.

mage studied here are represented by shallow craters in general, and the dimensions of the pits are far away from any comparable dimension of resonance of the radiation, it seems reasonable to use this simple approach, which yields satisfactory results.

Let us define the Oxyz-frame with the Oz-direction coinciding with the opposite to the normal to the initial surface of the specimen, which is represented by the Oxy-plane. The system of polar coordinates r, θ will be used in the following because of the angular symmetry of the pit. We assume that the intensity of the incident beam at the specimen surface has a Gaussian distribution of the form (see Fig. 7):

$$I = I_0 \exp\left(-\frac{r^2}{a^2}\right)$$

where I_0 is the on-axis intensity and a is the radial distance from the beam-axis to a 1/e intensity point. In the Fraunhofer approximation the scattered intensity in any θ=const plane, containing the Oz-axis, can be expressed by:

$$I_2 = \frac{I_0}{\lambda^2}\left|\int_{-\infty}^{\infty} A(r)\exp(-ikr\sin\theta)\,dr\right|^2 \qquad (14)$$

where:

$$A(r) = \exp\left(-\frac{r^2}{2a^2}\right) \qquad \text{for } |r| < r_0$$

$$A(r) = \exp\left(-\frac{r^2}{2a^2} - 2ikr_0\right) \qquad \text{for } |r| > r_0$$

and $2r_0$ the diameter of the defect.

By adding and subtracting the integral:

$$\int_{-r_0}^{r_0} \exp\left(-\frac{r^2}{2a^2} - ikr\sin\theta\right)dr \qquad (15)$$

within the absolute value signs, the integral in Eq. (14) can be converted into thr sum of two integrals, where the first integral extends from negative to positive infinity, whereas the second integral extends from from negative to positive infonity Carrying out the integration and the respective algebra,

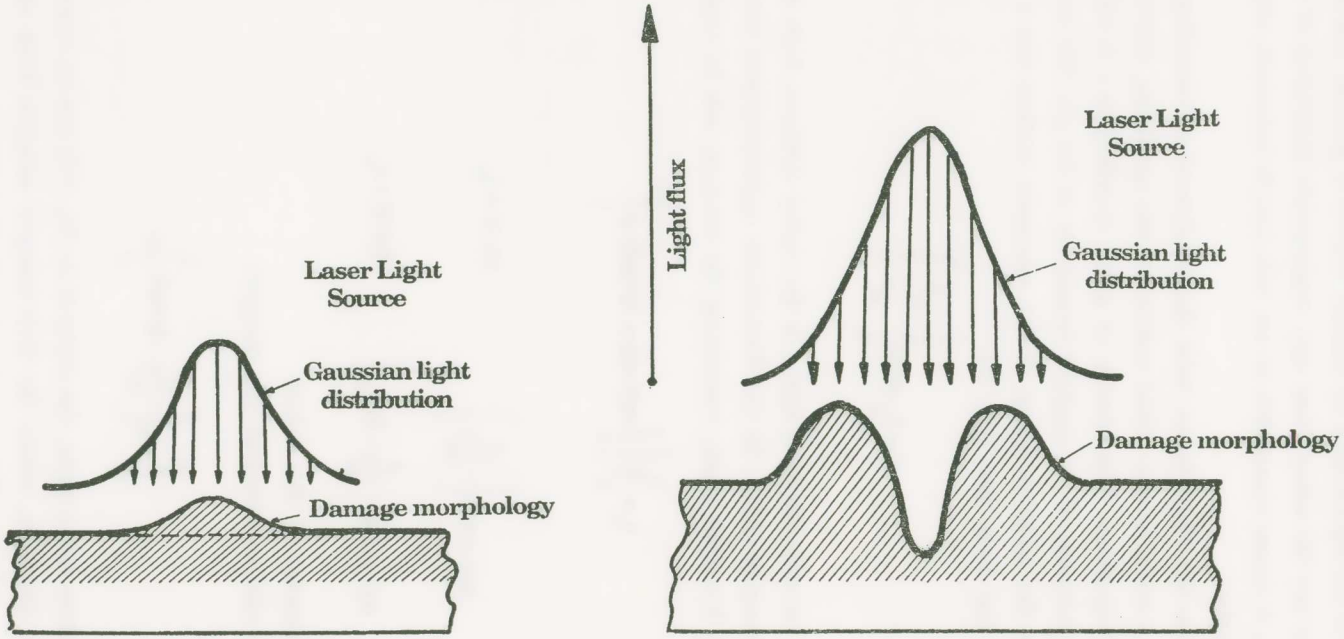

Fig. 7 The impinging light flux from a laser bundle and the damage morphology of the surface at the initial step of formation of the speckle (a) and after the development of the crater (b).

we obtain finally three terms, from which only the third one, corresponding to the diffraction of a Gaussian beam truncated by a pit, is not negligible. Using asymptotic expressions for the error functions appropriate for the case where $a \rangle\rangle r_0 \rangle \lambda$, $I(\theta)$ can be approximated by:

$$I(\theta) = E_0 \sin^2 kd \left[\frac{\sin (kr_0 \sin\theta)}{kr_0 \sin\theta} \right]^2 \tag{16}$$

where $E_0 = 32\pi a^2 r_0^2 I_0 / \lambda^2$.

Equation (16) represents the conventional single-defect diffraction pattern [5] with the overall intensity modulated by the pit depth.

When a small isolated quasi-circular defect is present in the illuminated spot on the surface the intensity I in a transverse plane passing through point 0_2 can be approximated by:

$$I(r) = I_a(r) + I_d(r) \tag{17}$$

where $I_a(r)$ is the background intensity distribution in thr absence of the defect and $I_d(r)$ is the intensity distribution pattern from the surface defect. The intensity distribution in the Fraunhofer diffraction pattern from the defect can be expressed by:

$$I_d(r) = I_0 \left[\frac{2 J_1 \left(\frac{2\pi r_0 r}{\lambda f} \right)}{\left(\frac{2\pi r_0 r}{\lambda f} \right)} \right]^2 \tag{18}$$

where I_0 is the intensity at the center of the pattern and $2r_0$ the diameter of the defect.

The intensity distribution $I_d(r)$ is a typical diffraction distribution shown schematically in Fig. 7. The $I_d(0) = I_0$ intensity is very small.

EXPERIMENTAL EVIDENCE OF FORMATION OF LASER SPECKLES

An experimental investigation of the formation of diffraction patterns and their rainbow caustics was undertaken in order to ascertain the theory developed. The experimental set-up used in the tests was simple. A Neon or

Argon gas cw-laser light beam was passing through a collimator and a diaphragm regulating the intensity of the light bundle. The light beam is impinging normally on the surface of the plexiglas specimen and the partly reflected from its surface light beam is received on a ground glass reference screen, or on the viewing frame of the recording camera.

By regulating the light intensity of the laser beam we adjust the light intensity of the impinging beam to be sufficient for creating a speckle of the flat surface of the plate. In order to facilitate the creation of the speckle phenomenon, coloured plexiglas plates were used, so that the almost totality of the impinging energy was acting on the surface of the specimen.

The formation of the speckle crater resulted in a progressive variation of the angle of incidence of the light rays in the zone of development of the speckle, which when reflected, formed an interferogram containing all information concerning the instantaneous shape of the crater and its evolution as the light flux from the laser beam was increased. Figures 8 and 9 present a series of interferograms indicating the development of the laser speckle on a flat surface of a coloured thin plexiglas plate. For a light flux emitted from the laser kept constant at some level, the interferogram started and interference fringes were created at the beginning of the process with a high speed, as the phenomenon of deformation of the surface accelerated at the beginning. As the process evoluted, the formation of fringes was retarded, tending to some limit, where the interferogram is stabilized corresponding to the respective level of light flux from the laser.

In the first steps of creation of the speckle, where the pit is formed by elastic deformations progressive reduction and withdrawal of the light flux of the laser reduced progressively the shape and number of fringes of the interferogram, up to its complete extinction (Fig. 8).

Increasing the level of the light flux beyond a certain limit, up to which the speckle deformation was elastic, permanent destortions of the shape of the surface of the plate were established. It was observed that it was a zone of light flux producing permanent deformations of the speckle, for which the respective interferogram was a continuous one with a smooth change of the interfringe distance (see Fig. 8b).

However, when another upper bound of light flux can be reached, for which a second more brillant interferogram was emerging from the center of the initial interferogram, this new interferogram was again progressively

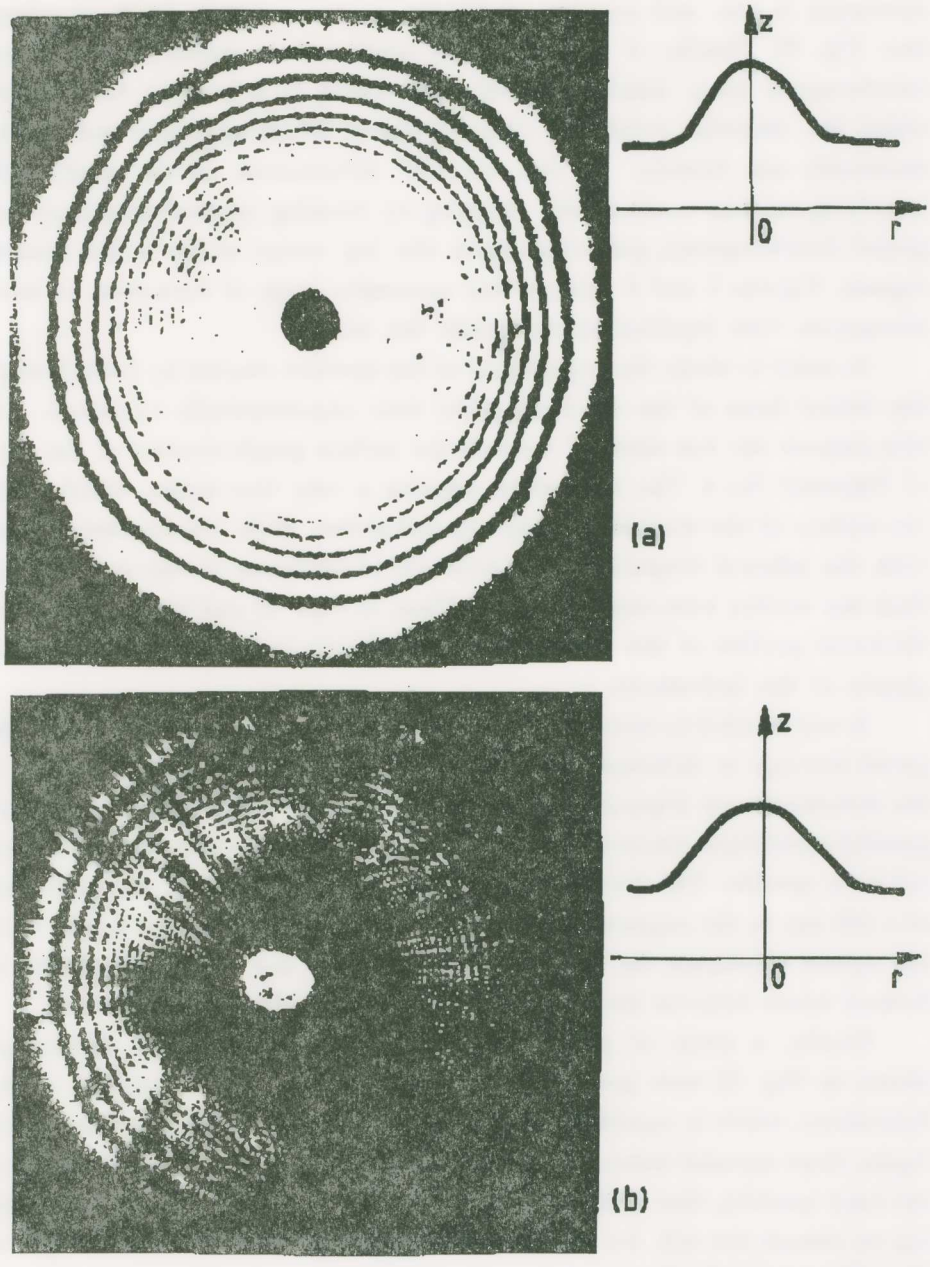

Fig. 8. Interferograms at the initial phase of creation of the protrusion and their respective shapes.

increasing in size and number of fringes, up to a certain limit of energy (sec. Fig. 9). Finally, if the light flux continued to increase, this second interferogram lying inside the first one, tended to a limiting form, above which the material eventually changed phase, becoming liquid and boiling drastically and fiercely. In this level of deformation of the speckle, the interferogram was continuously changing by forming internal secondary regional interferograms, pulsating inside the big crater of the stable interferogram. Figures 5 and 6 indicate the successive steps of formation of interferograms with liquified phases inside the craters.

In order to study the topography of the speckles created by laser damage the lateral faces of the deformed plate were experimentally examined. For this purpose use was made of a rectilinear surface graph-recorder of the type of Talytsurf No. 4. The instrument disposes a very fine stylus, which scans the surface of the workpiece along any radial line. With this instrument and with the selected magnification, variations of thickness of the order of less than one micron were easily detected. Thus, in Figs. 10 and 11 the respective thickness profiles of the corresponding interferograms were plotted from the graphs of the instrument.

It was decided to sweep the neighborhood of the speckle by parallel equispaced tracings in different orientations in order to create the relief map of the deformed zone. Figures 10 and 11 present the profile graphs of rectilinear parallel equidistant traverses for two different steps of development of a typical laser speckle. The first pattern in Fig. 11 corresponds to the formation of a hill due to the expansion of the material heated by the laser beam, while the second represents the later phase, when at the top of the hill a crater is formed where later-on the material of the plate is liquified.

Finally, a series of photographs with a scanning electron microscope shown in Fig. 12 were presented in an arrangement of z-modulation of the instrument, which is capable to present the topography of the scanned surface. Again, these scanned microphotographs present in relief the different shapes of the laser speckles, that is the speckle at its initial step of deformation presenting an almost flat hill, the second when a flat top is formed at the height of the hill, and finally the third step when a distinct crater is developed at the center of the hill.

This extensive experimental evidence corroborates the theory of creation of speckles under the influence of a laser light beam impinging normally on

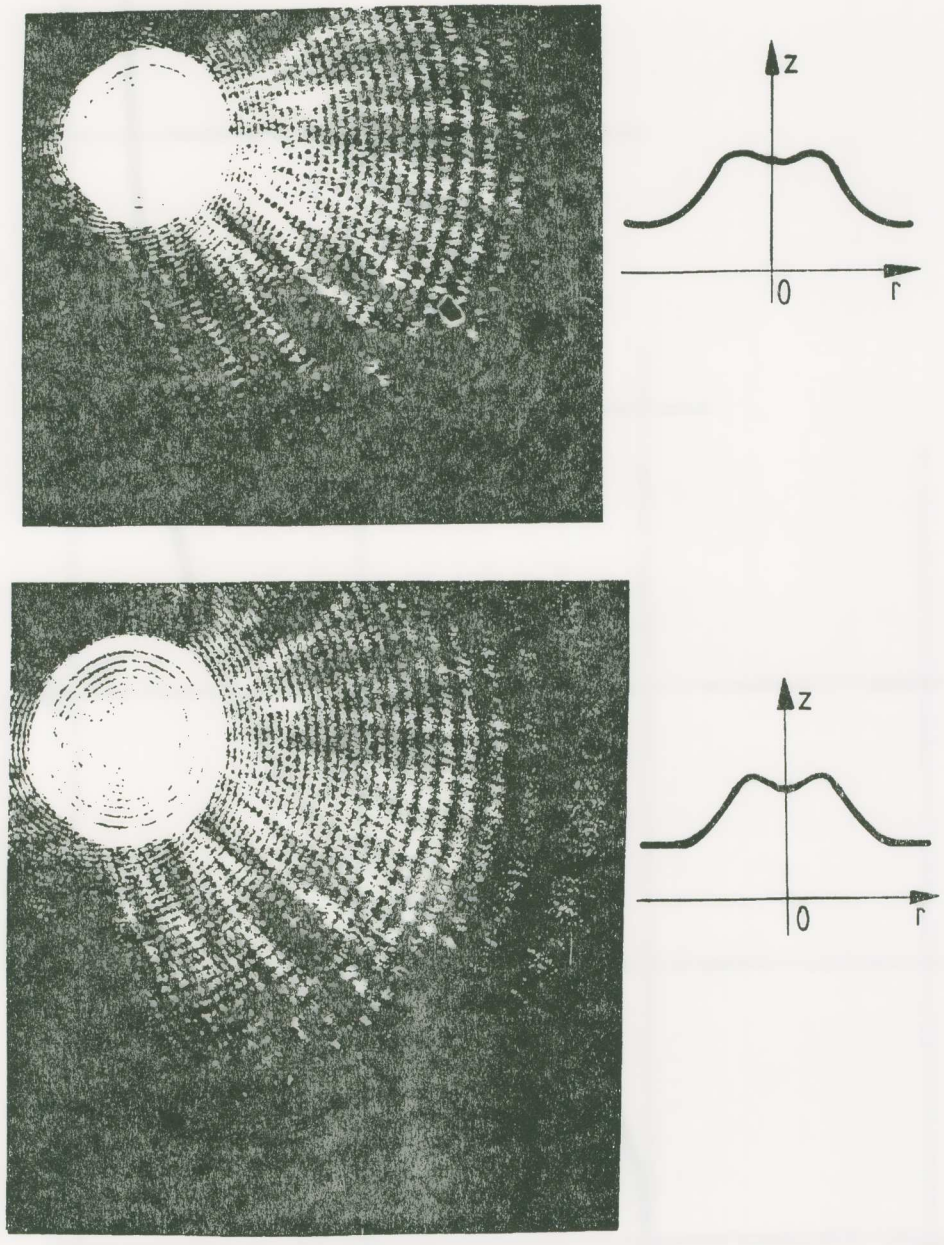

Fig. 9. Interferograms of the initial and subsequent phases of the phenomenon of creation of the speckle when a crater starts to develop.

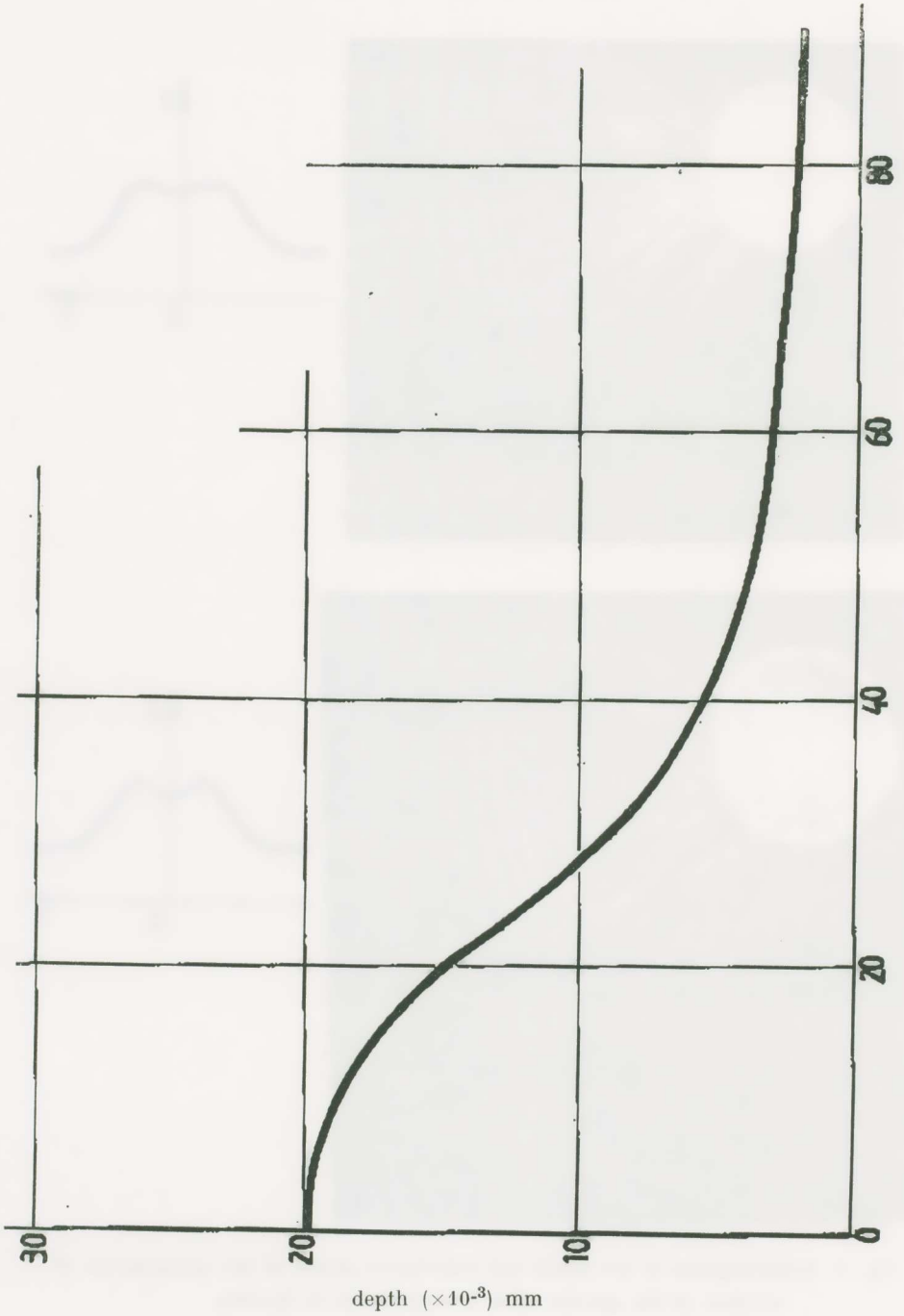

Fig. 10 The radial profile of the speckle.

the workpiece. The properties of the rainbow caustics predicted in the theory may be strickingly confirmed by the experiments with laser light damage.

The two dimensional space of deflections due to speckle defines the limiting curve shown in the figures, which is a classical rainbow caustic, showing cusps, whose positions are depending on the form of the crater of the speckle. While the scattering of light around the speckle is classically singular the effect of diffraction consists in a softening of the singularities as we recede from the cusps. Figures 4 to 6 indicate the formation of the diffraction patterns from reflections at neighbouring areas of speckles, consisting of the inner cusped rainbow caustic C_2, as well as the detailed patterns at the neighbourhoods of the cusps, where the quantized diffraction patterns are very distinct. While the internal rainbow caustic C_2 is a four-cusp curve, the external one C_1, is a smooth one. The distances Δx, Δy and Δc, given by relations (10), can be readily evaluated from the interferograms.

By rotating thr reference screen, where the interferograms are formed, so that the laser light bundle is impinging obliquely to the screen, a transformation of the caustic pattern is achieved, where, for small angles of rotation the rainbow caustics become elliptically formed (see Fig. 5). If the angle of angular displacement of the screen is increased, the pattern becomes very complicated, as it is indicated in Fig. 6, since the configuration on the screen corresponds to an oblique intersection of the caustic pattern in space. In this configuration zones corresponding to a value of the pertrubation parameter, $\varepsilon=0$, appear as very restricted areas. The similarity of the experimentally obtained pattern of Figs. 4 to 6 with the configuration of a typical *hyperbolic umbilic catasctrophe* in Fig. 1 is striking, thus, confirming the idea that the rainbow caustics correspond to intersections of the rainbow caustic surface in space by different planes and this caustic surface belongs to the category of the *hyperbolic umbilic catastrophes.*

Then, the shapes of the rainbow caustics can give detailed information about the form of the speckle created by the laser light damage, by defining the varation of the values of Δx, Δy, Δc for different intersections of the rainbow caustic surface by different planes $\varepsilon=\varepsilon_i$. In practice, the details of curves C become blurred to a different degree, depending on the choice of the value of the perturbation parameter ε. Furthermore, in a finer scale it is also possible to observe the beginning of quantization of the rainbow caustic into diffraction spots, which occurs because the laser beam illuminates several unit cells in the speckle.

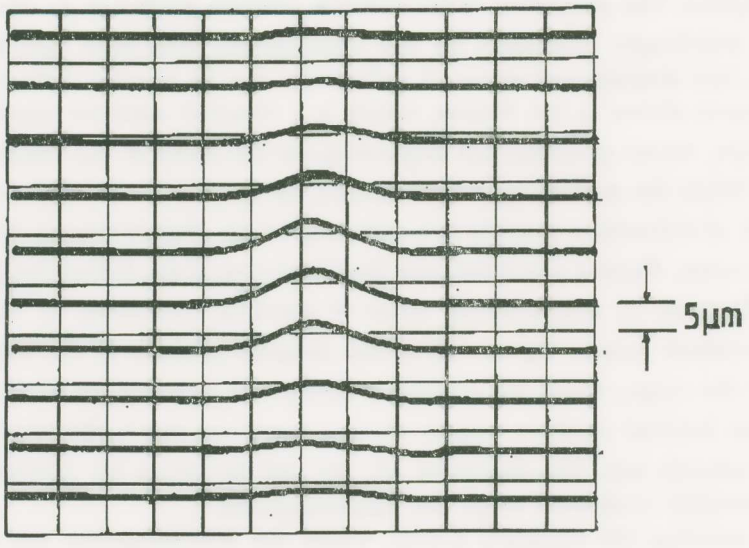

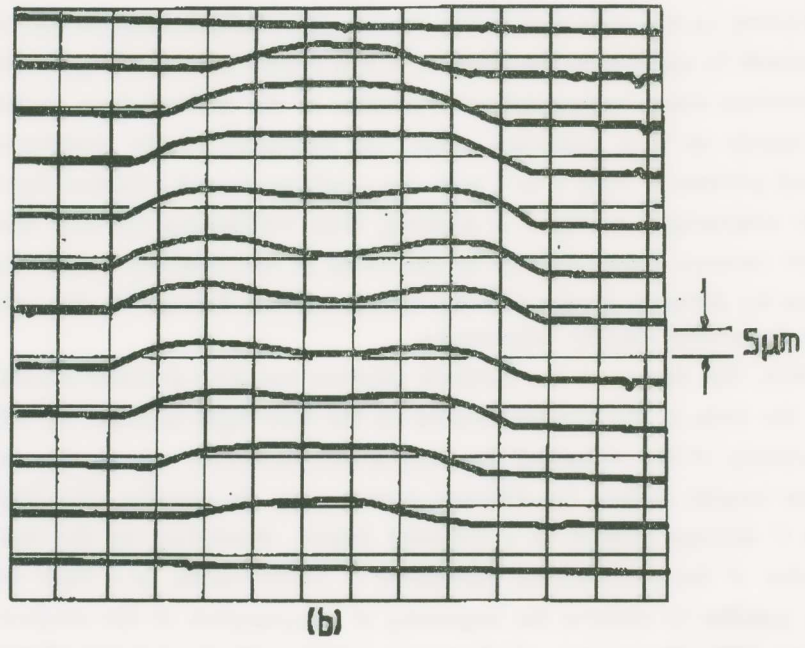

Fig. 11. Talysurf tracings of the variation of the thickness of the speckle hill by successive traverses (a) initical step (b) step with crater.

(a)

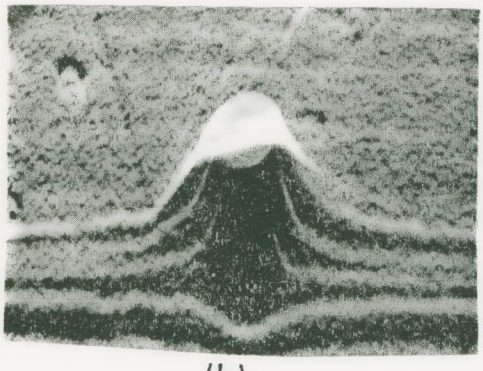

(b)

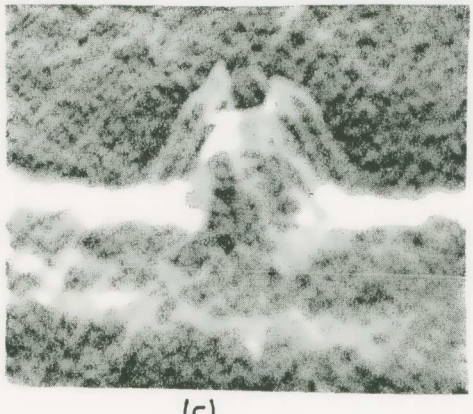

(c)

Fig.12 Interferograms of the speckle during the attack of the laser light as they are seen by a scanning electron microscope at z-modulation (a) initial step (b) initiation of crater (c) development of crater.

ACKNOWLEDGEMENT

The reserch programme pressent in this paper was partly supported by the Athens National Technical University and the National Academy of Athens reserch funds. The author expresses his appreciation for this generous support. He is also indebted to his secretary Mrs. Anny Zografaki for her help in typing and drawing the figures of this manuscript. Mr Alex Koutsambessis, Technician at the Laboratory for Testing Materials of the Athens National Technical University assisted during the execution of all experiments undertaken in this research programme. The author expresses his wholehearted thanks for this help.

REFERENCES

1. J. P. Toennies, *Applied Physics*, Vol. **3**, pp. 91-114 (1974).

2. U. Garibaldi, A. G. Levi, R. Spadacini and G. E. Tommei, Surface Science (1974).

3. J. N. Smith Jr., D.R. O'Keefe. H. Salgburg and R. L. Palmer, *Jnl. of Chemical Physics*, Vol. **50**, pp. 4667-4671 (1969).

4. M. V. Berry, *Jnl. of Physics A* (Math. Gen.), Vol **8**(4), pp. 566-584. (1975).

5. M. Born and E. Wolf, «*Principles of Optics*» 5th Edition (Pergamon Press London) (1975).

6. J. C. Maxwell, *Philosophical Magazine*, Vol. **40**, 54, pp. 421-427 (1870).

7. R. Thom, *Stabilité structurelle et Morphogênese*, New York, Benjamin (1972).

8. H. Abramowitz and A. Stegun, *Handbook of Mathematical Functions*, (U.S. Bureau of Standards Wash. D.C.) (1964).

9. G.B. Airy, *Proceed. Cambridge Phil. Soc.*, Vol **6**, pp. 379-402 (1838).

10. K. W. Ford and J. A. Wheeler, *Annal. Phys.*, NY **7**, pp. 259-322 (1959).

11. T. Pearcey, *Phil. Magazine*, Vol. **37**, pp. 311-317 (1946).

12. P. S. Theocaris and J. Michopoulos, *Applied Optics*, Vol. **21** (6), pp. 1080-1092 (1982).

13. P.S. Theocaris, «Francisco Maurolyco, a precursor of Newton and Kepler. Four hundred years from the date of his death», *Proceed. Nat. Acad. of Athens*, Vol. **53** (no.2), pp. 110-127 (1978).

ΠΕΡΙΛΗΨΙΣ

Μελέτη τῆς τοπολογίας ἐπιφανειῶν ὑπὸ τὴν ἐπίδρασιν ἀκτίνων Laser

Εἰς τὴν ἀνακοίνωσιν αὐτὴν μελετᾶται ἡ μορφὴ στιγμάτων δημιουργουμένων ἐπὶ λείων ἐπιφανειῶν προσβαλλομένων ὑπὸ ἀκτίνων Laser. Ἡ μορφολογία καὶ αἱ χαρακτηριστικαὶ διαστάσεις τῶν δημιουργουμένων στιγμάτων τοιούτων καταστροφῶν μελετῶνται κατὰ τὴν ἐξέλιξιν τοῦ φαινομένου προσβολῆς τῆς ἐπιφανείας ὑπὸ τῶν ἀκτίνων Laser τῇ βοηθείᾳ ὀπτικῶν μεθόδων συμβολομετρίας καὶ περιθλάσεως τῶν προσπιπτουσῶν ἀκτίνων. Ἀποδεικνύεται διὰ πρώτην φορὰν ὅτι τὰ δημιουργούμενα συμβολογράμματα ἐκ τῆς παραμορφουμένης ἐπιφανείας σχηματίζουν ἀπεικονίσεις συμβολῆς, δημιουργοῦντα καυστικάς, ἤτοι καταστροφὰς ἀνωτέρας τάξεως τοῦ τύπου τῶν *ὑπερβολικῶν ὀμφαλοειδῶν ἐπιφανειῶν*, συμφώνως πρὸς τὴν κλαστικὴν μαθηματικὴν θεωρίαν καταστροφῶν τοῦ René Thom [7].

Αἱ ἐπιφάνειαι αὐταὶ τεμνόμεναι ὑπὸ ἐπιπέδων καθέτων πρὸς τὸν ἄξονα τῆς ὀπτικῆς δέσμης σχηματίζουν δύο καμπύλας, τὰς καλουμένας *ἴχνη οὐρανίου τόξου*, διότι οἱ νόμοι δημιουργίας των εἶναι οἱ αὐτοὶ μὲ τοὺς νόμους τοὺς διέποντας τὴν δημιουργίαν τῶν γνωστῶν οὐρανίων τόξων εἰς τὴν ἀτμοσφαῖραν, φαινόμενα τὰ ὁποῖα πρῶτος ἐμελέτησεν καὶ ἔδωκε τὴν ὀρθὴν λύσιν τοῦ φαινομένου των ὁ Ἕλλην σοφὸς Φραγκίσκος Μαυρόλυκος πρὸ τοῦ ἔτους 1575, ἔτους τοῦ θανάτου τοῦ σοφοῦ [13].

Τὰ ἴχνη οὐρανίου τόξου ἀποτελοῦνται ἀπὸ διπλῆν καμπύλην, τὴν μίαν ἐντὸς τῆς ἄλλης. Ἐνῶ ἡ ἐξωτερικὴ εἶναι λεία προσομοιάζουσα πρὸς κύκλον ἢ ἔλλειψιν, ἡ ἐσωτερικὴ εἶναι *ραμφοειδὴς τετράσκελος καμπύλη* μὲ τὰ ράμφη ἐστραμμένα πρὸς τὰ ἔξω. Αἱ ἀποστάσεις, εἴτε τῶν κορυφῶν τῶν ραμφῶν, εἴτε τῶν κοιλιῶν τῶν τεσσάρων καμπύλων, ἀπὸ τῆς ἐξωτερικῆς καυστικῆς δίδουν σχέσεις, δι' ὧν ὑπολογίζεται ἐπακριβῶς τὸ ὕψος καὶ ἡ μορφολογία τῶν στιγμάτων των καταστροφῶν ἐξ ἀκτίνων Laser.

Κατὰ τὴν περίπτωσιν τῆς συγκεντρωμένης δέσμης τῶν ἀκτίνων ἐπὶ τῆς λείας ἐπιφανείας τοῦ δοκιμίου δημιουργεῖται τοπικὴ συγκέντρωσις ἐνεργείας εἰς τὸ σημεῖον προσπτώσεως, ἔχουσα ὡς ἀποτέλεσμα τὴν θέρμανσιν τῆς περιοχῆς καὶ τὴν διόγκωσίν της, δημιουργοῦσα λόφον, τοῦ ὁποίου τὰ χαρακτηριστικὰ μεγέθη ὑπολογίζονται ἐκ τῆς ἀρχικῆς συμβολῆς τῶν ἀνακλωμένων ἀκτίνων, αἱ ὁποῖαι σχηματίζουν ἐπὶ πετάσματος συμμετρικὸν κυκλικὸν συμβολόγραμμα.

Ἐὰν ἡ προσπίπτουσα ἐνέργεια ὑπερβαίνῃ ὡρισμένην στάθμην καὶ χρόνον προσπτώσεως, ὁ σχηματιζόμενος λόφος ἐξελίσσεται εἰς κρατῆρα ἡφαιστείου, εἰς τὸ κέντρον αὐτοῦ. Αἱ ἀνακλώμεναι ἀκτῖνες ἐκ τοῦ κρατῆρος τούτου δημιουργοῦν δεύτερον συμβολόγραμμα, φωτεινότερον τοῦ πρώτου, καὶ ὁμόκεντρον μὲ τὸ πρῶτον. Ἐξέλιξις

τῶν δύο συμβολογραμμάτων δημιουργεῖ ἐν συνεχείᾳ τὰς ἀπεικονίσεις περιθλάσεως μὲ τὰς χαρακτηριστικὰς καμπύλας οὐρανίου τόξου.

Αἱ διαδοχικαὶ φάσεις τοῦ φαινομένου δημιουργίας τοῦ στίγματος Laser μελετῶνται, αἱ μὲν δύο πρῶται ἐπὶ τῇ βάσει τῆς ὀπτικῆς θεωρίας συμβολῆς Fraunhofer, ἡ δὲ τελευταία βάσει τῆς θεωρίας καταστροφῶν καὶ τῆς ἁπλοποιημένης θεωρίας περιθλάσεως κατὰ Kirchhoff, ἡ ὁποία ἔχει ἐφαρμογὴν δι' ἀραιὰς διαταραχὰς τῆς ἐπιπέδου λείας ἐπιφανείας, ὡς εἶναι ἡ περίπτωσις ὑπὸ ἐξέτασιν. Ἡ προσπίπτουσα ἀκτινοβολία Laser θεωρεῖται παρουσιάζουσα ἁπλῆν κατανομὴν ἐν τῷ χώρῳ κατὰ Gauss.

Πειραματικαὶ μελέται μὲ ἁπλᾶς διατάξεις ἰσχυούσας διὰ τὴν θεωρίαν Fraunhofer ἔδωκαν συμβολογράμματα μεγάλης πιστότητος καὶ εὐαισθησίας. Αἱ αὐταὶ διατάξεις ἐχρησιμοποιήθησαν καὶ διὰ τὴν μελέτην τῶν φαινομένων περιθλάσεως.

Πρὸς διασταύρωσιν τῶν ἀποτελεσμάτων ἐκ τῶν ὀπτικῶν πειραματικῶν μεθόδων ἐγένετο ἐν συνεχείᾳ δι' ἕκαστον πείραμα μελέτη τῆς τοπογραφίας τοῦ στίγματος, τῇ βοηθείᾳ λίαν εὐαισθήτων μηχανημάτων αὐτομάτου καταγραφῆς τῶν ἀνωμαλιῶν τῆς ἐπιφανείας, διὰ σαρώσεώς της μὲ λίαν λεπτὸν καὶ εὐαίσθητον στύλον τοπογραφικοῦ μηχανήματος τύπου Talysurf No. 4. Τὰ ἐν λόγῳ διαγράμματα ἀπέδειξαν τὴν συμφωνίαν τῶν θεωρητικῶν ἀποτελεσμάτων καὶ τῶν ὀπτικῶν τοιούτων. Τέλος, μελέτη τῶν στιγμάτων διὰ τοῦ ἠλεκτρονικοῦ μικροσκοπίου σαρώσεως τοῦ ἐργαστηρίου Ἀντοχῆς Ὑλικῶν τοῦ Ε. Μ. Πολυτεχνείου, εἰς διαμόρφωσιν τοῦ ὀργάνου κατὰ τὴν z-κατεύθυνσιν προσπτώσεως τοῦ φωτὸς Laser, ἔδωκε συμβολογράμματα ταυτόσημα μὲ τὰ εὑρεθέντα διὰ τῶν λοιπῶν μεθόδων. Ἡ τοιαύτη ταυτότης τῶν ἀποτελεσμάτων καταδεικνύει τὴν ἀκρίβειαν καὶ τὴν μεγάλην εὐαισθησίαν τῆς μεθόδου, ἡ ὁποία εἶναι ἡ πρώτη καθ' ὅσον γνωρίζομεν ἐφαρμογὴ τῆς μεθόδου τῆς συμβολομετρίας διὰ τὴν μελέτην τῶν διαδικασιῶν ἐφαρμογῆς τῶν ἀκτίνων Laser εἰς συγκολλήσεις ἢ διατρήσεις καὶ ἐν γένει διαμορφώσεις, τόσον εἰς τὰ ἄψυχα ὑλικά, ὅσον καὶ εἰς τὴν ἔμβιον ὕλην.

Τέλος, δέον ὅπως ἀναφερθῇ ὅτι διὰ συνεχίσεως τῆς προσβολῆς τῆς ἐπιφανείας τοῦ δοκιμίου ὑπὸ τῆς συγκεντρωμένης δέσμης Laser, ἐφ' ὅσον ἡ ροὴ τῆς ὀπτικῆς ἐνεργείας εἶναι ὑπεράνω κρισίμων ὁρίων, μετὰ τὴν πλήρη ἀνάπτυξιν τοῦ κρατῆρος εἰς τὴν διαταραχήν, δημιουργεῖται τῇξις τοῦ ὑλικοῦ ἐντὸς τοῦ κρατῆρος καὶ ἐν συνεχείᾳ ἔντονος βρασμὸς τῆς τακείσης ὕλης. Διὰ τοῦ τρόπου αὐτοῦ ὁ κρατὴρ προχωρεῖ εἰς τὸ βάθος τῆς πλακὸς μέχρι πλήρους διατρήσεώς της. Ἡ διαδικασία αὐτὴ ἀποτελεῖ τὸν βασικὸν μηχανισμὸν διαμορφώσεως τῶν σωμάτων ἐξ ἀποστάσεως διὰ χρήσεως φωτὸς Laser, μεθόδου ἡ ὁποία ἔχει εὕρει σήμερον εὐρείας ἐφαρμογὰς εἰς τὴν τεχνολογίαν καὶ τὴν ἰατρικήν.